Electronic Supplementary Material (ESI) for Physical Chemistry Chemical Physics

Supplementary Information

Atomic selectivity in dissociative electron attachment to dihalobenzenes

Namdoo Kim,[a] Taeil Sohn,[a] Sang Hak Lee,[a ‡] Dhananjay Nandi[a §] and Seong Keun Kim[a b *]

[a] *Department of Chemistry, Seoul National University, Seoul 151-747, Korea*

[b] *WCU Department of Biophysics and Chemical Biology, Seoul National University, Seoul 151-747, Korea*

---

‡ Current address: Department of Physics, University of Illinois at Urbana-Champaign, Urbana, Illinois 61801-3080, USA

§ Current address: Indian Institute of Science Education and Research - Kolkata, Mohanpur - 741252, Nadia, West Bengal, India

* To whom correspondence should be addressed: Electronic mail: seongkim@snu.ac.kr. Tel.: +82-2-880-6659. Fax: +82-2-889-5719

		Cl	Ring	Br
2-BCB	neutral	-0.375	0.046	0.329
	anion	-0.429	0.078	-0.649
3-BCB	neutral	-0.364	0.192	0.172
	anion	-0.458	0.234	-0.776
4-BCB	neutral	-0.353	0.140	0.213
	anion	-0.437	0.210	-0.773

TABLE S1. Mulliken atomic charges for the three isomers of BCB calculated at the MP2/aug-cc-pVDZ level. Most of the negative charge (0.95 ~ 0.98 *e*) is invested on the *less* electronegative Br atom upon electron attachment, which undergoes a drastic change from a positively charged moiety in the neutral to the strongest negatively charged one in the anion.

		Br	Ring	I
2-BIB	neutral	0.036	-0.258	0.222
	anion	-0.090	-0.220	-0.690
3-BIB	neutral	0.013	-0.205	0.192
	anion	-0.106	-0.136	-0.758
4-BIB	neutral	0.014	-0.206	0.192
	anion	-0.105	-0.212	-0.683
		Cl	Ring	I
2-CIB	neutral	-0.067	-0.164	0.231
	anion	-0.181	-0.224	-0.5954
3-CIB	neutral	-0.086	-0.110	0.196
	anion	-0.186	-0.156	-0.658
4-CIB	neutral	-0.083	-0.112	0.195
	anion	-0.184	-0.133	-0.683

TABLE S2. Mulliken atomic charges of the three isomers of BIB and CIB calculated at the MP2/LanL2DZ level. Here, it is the I atom, again the *least* electronegative moiety, that undergoes the most drastic change in atomic charge upon electron attachment.

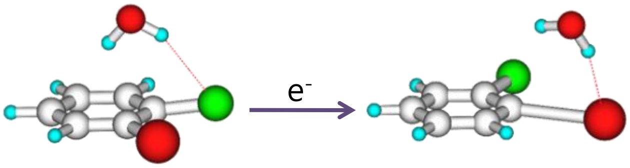

FIG. S1. Optimized structures of [2-BCB-$(H_2O)_1$] and [2-BCB-$(H_2O)_1$]$^-$. In the neutral state, an H atom of water directly interacts with Cl, which is the only negatively charged moiety in 2-BCB. In the anionic state, water moves toward the Br atom for a more preferential interaction, with its H atom forming a tighter bond with Br, which accommodates most of the negative charge in electron attachment. Note the C–Br bond is significantly elongated in BCB$^-$.

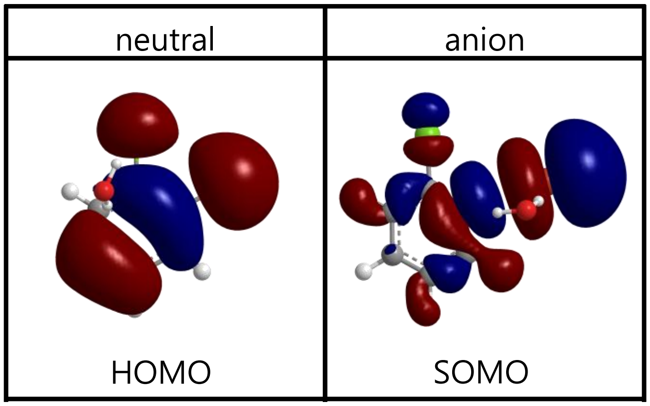

FIG. S2. Neutral HOMO and anionic SOMO of $[2\text{-BCB-}(H_2O)_1]^-$. Cl and Br are colored green and red, respectively. Water interacts directly with Cl in the neutral but switches to a preferential interaction with the Br-end in the anion. Calculations were carried out using Gaussian 03, revision C.02 with B3LYP/6-311++G**.

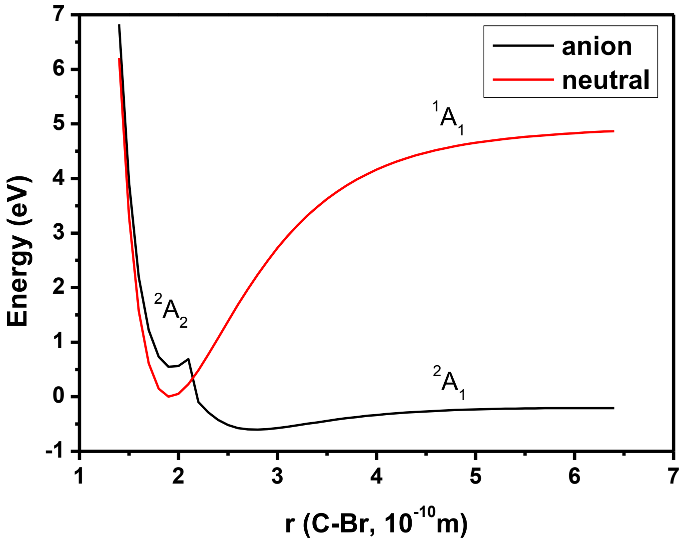

FIG. S3. Calculated potential energy curves of 4-BCB. The energies were calculated as a function of the C–Br distance from 1.4 to 6.4 Å. There is a curve-crossing between two anionic potential energy curves ($^2A_2$ and $^2A_1$) at ~2.0 Å, after which the $^2A_1$ state becomes the anionic ground state with a shallow minimum at ~2.5 Å. The neutral ground state (also of A_1 symmetry) is lower in energy than even the anionic $^2A_2$ state at short distances, but quickly rises in energy as the C–Br distance increases. Calculations were carried out using Gaussian 03, revision C.02 at the B3LYP/6-311++G** level.

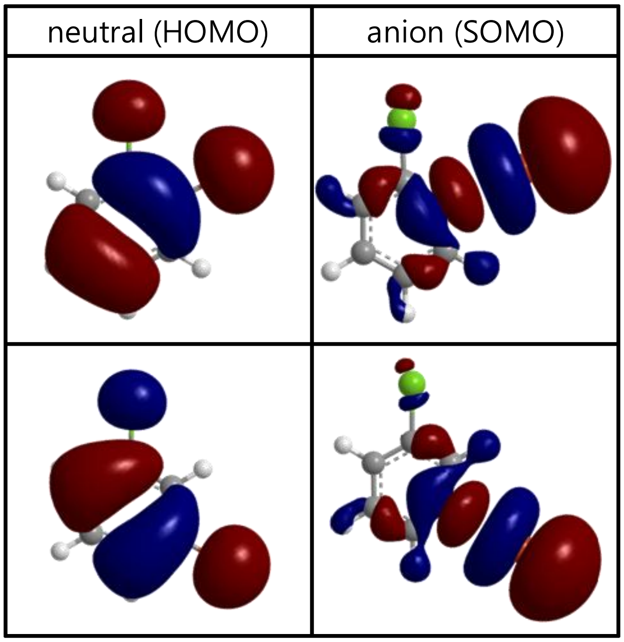

FIG. S4. Neutral HOMO and anionic SOMO of 2-BCB (top) and 3-BCB (bottom). Cl and Br are colored green and red, respectively. The HOMO of the neutral molecule is a non-bonding orbital, with a node between C and Br. The SOMO of the anion is highly developed around the Br moiety, as in the case of 4-BCB (Fig. 5 of the main text). Calculations were carried out using Gaussian 03, revision C.02 at the MP2/aug-cc-pVDZ level.

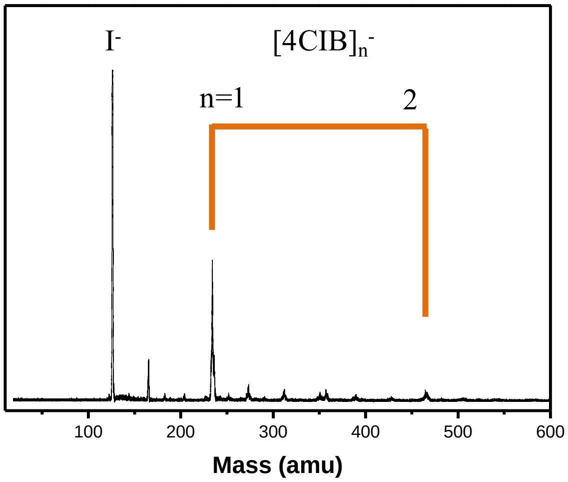

FIG. S5. Mass spectrum of 4-CIB cluster anions. The most intense peak is due to I^-, with the cluster anions trailing in intensity in a rapidly decreasing manner.

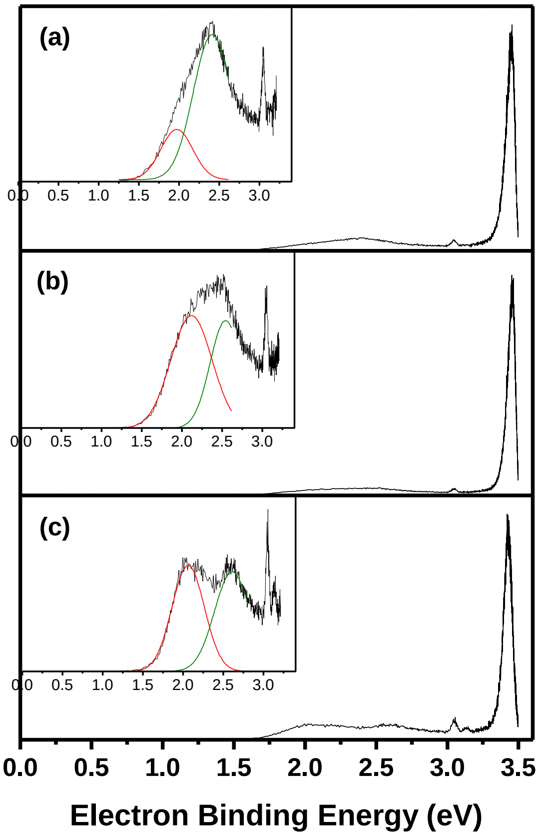

FIG. S6. Photoelectron spectrum of (a) 2-CIB, (b) 3-CIB and (c) 4-CIB monomer anions. The sharp atomic photoelectron band of I$^-$ at 3.06 eV is due to a two-photon process involving photodissociation followed by photodetachment. As in the case of BCB, the broad photoelectron spectrum from 1.5 to 3.0 eV can be deconvoluted into two Gaussian bands separated by ~0.5 eV.

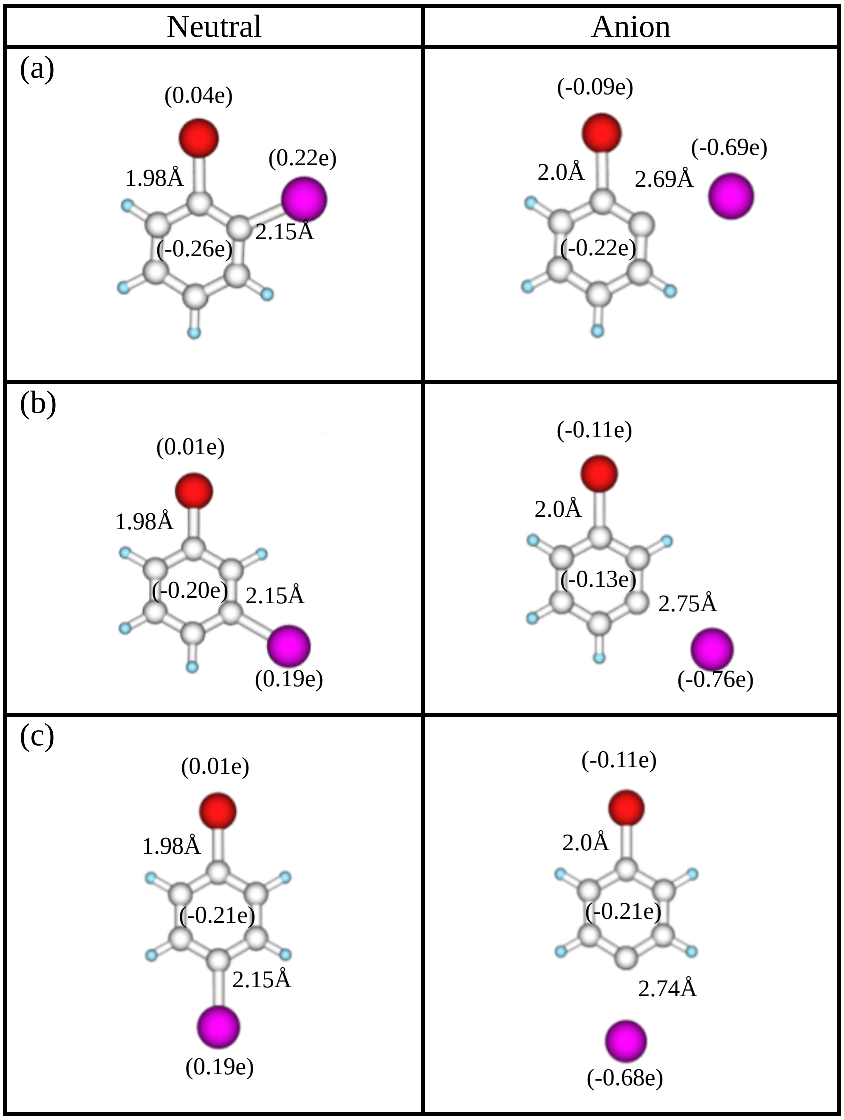

FIG. S7. Optimized geometries for the three isomers of neutral and anionic BIB. Br and I are colored red and purple, respectively. The C–Br bond length increases drastically from 2.2 to 2.7 Å upon electron attachment, indicating the anti-bonding nature of the SOMO localized around the C–Br bond. Most of the approaching electron's charge (87 ~ 95%) goes to the I atom. Note that neither halogen atom has a negative charge in neutral BIB.

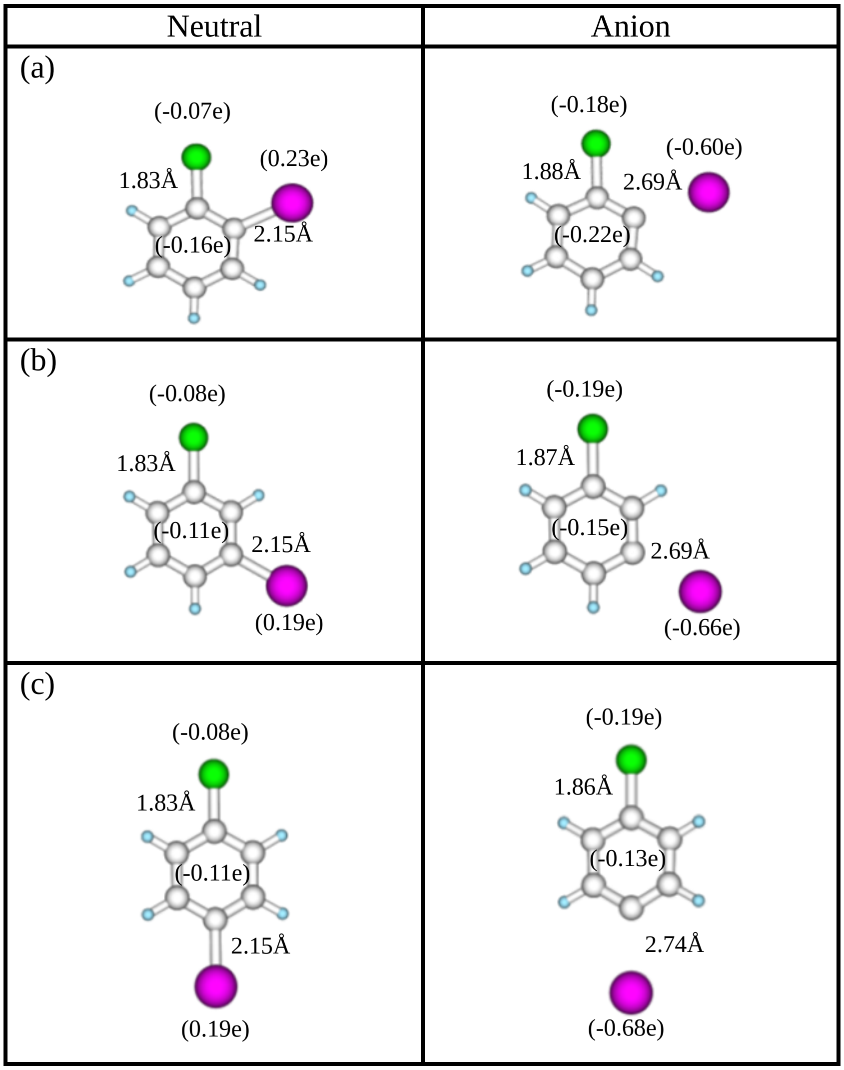

FIG. S8. Optimized geometries for the three isomers of neutral and anionic CIB. Cl and I are colored green and purple, respectively. As with BIB, the C–I bond length increases drastically from 2.2 to 2.7 Å upon electron attachment, and most of the approaching electron's charge (83 ~ 87%) goes to the I atom.

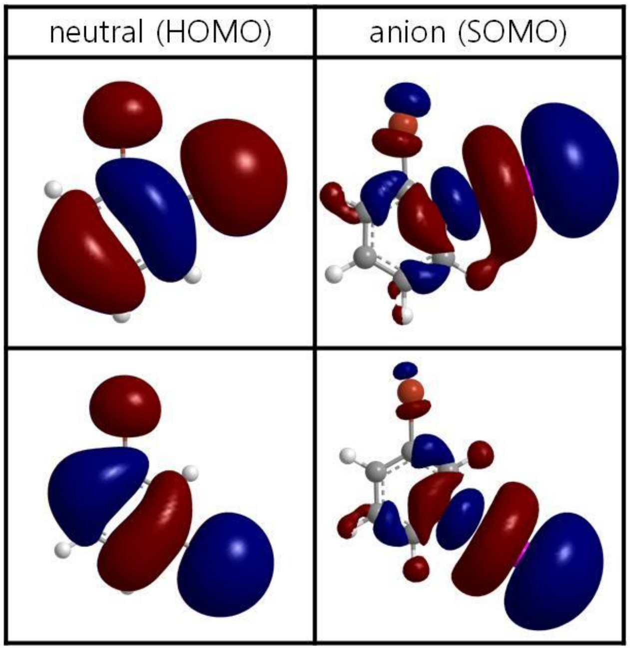

FIG. S9. Neutral HOMO and anionic SOMO of 2-BIB (top) and 3-BIB (bottom). Br and I are colored red and purple, respectively. The HOMO of the neutral molecule is a non-bonding orbital, with a node between C and I. The SOMO of the anion is highly developed around the I moiety. Calculations were carried out using Gaussian 03, revision C.02 at the MP2/LanL2DZ level.

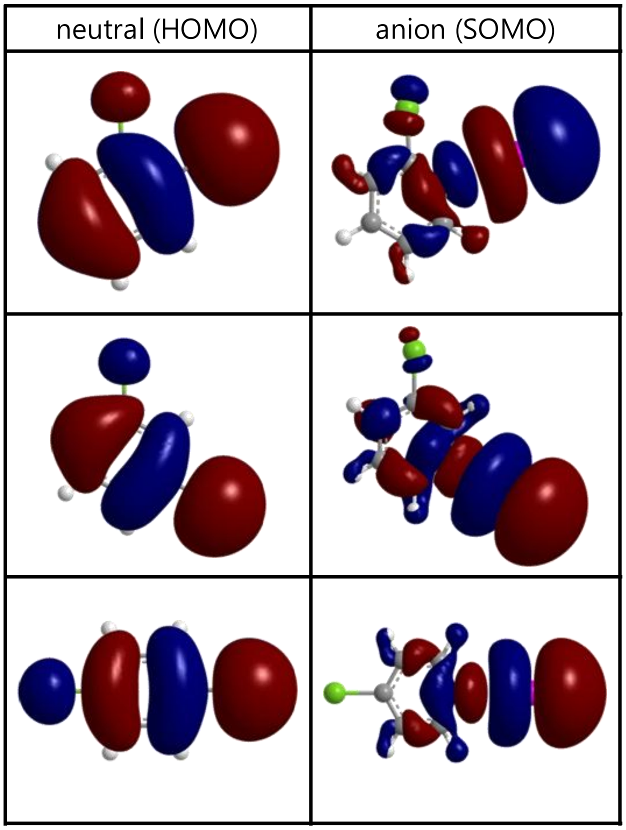

FIG. S10. Neutral HOMO and anionic SOMO of 2-CIB (top), 3-CIB (middle), and 4-CIB (bottom). Cl and I are colored green and purple, respectively. The HOMO of the neutral molecule is a non-bonding orbital, with a node between C and I. The SOMO of the anion is highly developed around the I moiety. Calculations were carried out using Gaussian 03, revision C.02 at the MP2/LanL2DZ level.

(11) Frisch, M. J.; Trucks, G. W.; Schlegel, H. B.; G. E. Scuseria; Robb, M. A.; Cheeseman, J. R.; J. A. Montgomery, J.; T. Vreven; Kudin, K. N.; Burant, J. C.; Millam, J. M.; Iyengar, S. S.; Tomasi, J.; Barone, V.; Mennucci, B.; Cossi, M.; Scalmani, G.; Rega, N.; Petersson, G. A.; Nakatsuji, H.; Hada, M.; Ehara, M.; Toyota, K.; Fukuda, R.; Hasegawa, J.; Ishida, M.; Nakajima, T.; Honda, Y.; Kitao, O.; Nakai, H.; Klene, M.; Li, X.; Knox, J. E.; Hratchian, H. P.; Cross, J. B.; Adamo, C.; Jaramillo, J.; Gomperts, R.; Stratmann, R. E.; Yazyev, O.; Austin, A. J.; Cammi, R.; Pomelli, C.; Ochterski, J. W.; Ayala, P. Y.; Morokuma, K.; Voth, G. A.; Salvador, P.; Dannenberg, J. J.; Zakrzewski, V. G.; Dapprich, S.; Daniels, A. D.; Strain, M. C.; Farkas, O.; Malick, D. K.; Rabuck, A. D.; Raghavachari, K.; Foresman, J. B.; Ortiz, J. V.; Cui, Q.; Baboul, A. G.; Clifford, S.; Cioslowski, J.; Stefanov, B. B.; Liu, G.; Liashenko, A.; Piskorz, P.; Komaromi, I.; Martin, R. L.; Fox, D. J.; Keith, T.; Al-Laham, M. A.; Peng, C. Y.; Nanayakkara, A.; Challacombe, M.; Gill, P. M. W.; Johnson, B.; Chen, W.; Wong, M. W.; Gonzalez, C.; Pople, J. A., Gaussian 03, Revision C.02; Gaussian, Inc: Wallingford CT, 2004